ELSEVIER

Solid State Ionics 152–153 (2002) 455–462

SOLID STATE IONICS

www.elsevier.com/locate/ssi

Synthesis and characterization of copper-stabilized zirconia as an anode material for SOFC

Mohan K. Dongare [a,*], Avinash M. Dongare [b], V.B. Tare [c], Erhard Kemnitz [d]

[a] *Catalysis Division, National Chemical Laboratory, Pune 411008, India*
[b] *Government College of Engineering, Pune, India*
[c] *Engineering College, Bharati Vidyapith, Pune, India*
[d] *Institute of Chemistry, Humboldt University, Hessiche Strase 1-2, Berlin, Germany*

Accepted 20 January 2002

Abstract

Solid oxide fuel cells (SOFC) are now being seriously considered for alternate energy source because of the environmental hazards associated with the use of fossil fuels and their limited availability. As a part of the development of these fuel cells, we have synthesized a series of $CuO-ZrO_2$ samples with varying concentration of CuO. In this paper, we present the study of copper-stabilized zirconia as an anode material in SOFC. The role of copper oxide in stabilizing zirconia and the possible reasons for the increase in catalytic activity of the relevant composition have been discussed using the experimental data.

Keywords: Fuel cell; Anode; Stabilized zirconia; AC conductivity; Methane oxidation

1. Introduction

Solid oxide fuel cells (SOFC) are now being seriously considered for alternate energy source because of the environmental hazards associated with the use of fossil fuels and their limited availability. Recently, Gorte et al. [1] have demonstrated the possibility of manufacturing SOFC using direct oxidation of dry hydrocarbons with Cu–ceria-based anodes without the need of reforming. Kundakovic and Flytzani-Stephanopoulos [2] investigated the reduction kinetics of CuO in zirconium oxide systems and showed that 15% Cu in yttria-doped zirconia was most effective in complete oxidation of CH_4 in the temperature range of 570–825 K. Copper oxide catalysts supported on ZrO_2 have been used for total oxidation of CO by Zhou et al. [3]. They have reported that $CuO-ZrO_2$ showed better oxidation activity than other catalysts because of the easy reduction of highly dispersed copper species on ZrO_2. Recently, Dongare et al. [4] reported oxygen activity and ^{18}O-isotope exchange behaviour of copper-stabilized zirconia. In spite of these investigations suggesting the possible use of Cu based ZrO_2 as anode materials for SOFC, the role of CuO in enhancing the catalytic activity is not clearly understood. As a part of the development of fuel cells, we have synthesized a series of $CuO-ZrO_2$ samples with varying concentration of CuO. In this paper, we present the study of copper-stabilized zirconia as an

* Corresponding author. Tel.: +91-20-5893761; fax: +91-20-5893761.
E-mail address: dongare@cata.ncl.res.in (M.K. Dongare).

0167-2738/02/$ - see front matter © 2002 Elsevier Science B.V. All rights reserved.
PII: S0167-2738(02)00371-5

anode material in SOFC. The role of copper oxide in stabilizing zirconia and the possible reasons for the increase in catalytic activity of the relevant composition have been discussed using the experimental data.

2. Experimental

2.1. Preparation of $CuO-ZrO_2$ samples

Samples of Cu-stabilized zirconia were prepared employing the sol–gel technique. The resulting glassy solid was ground to a fine powder and subsequently heat-treated at different temperatures to study the X-ray structure and phase transformations. The samples were heated for 12 h at 623, for 12 h at 773, and for another 12 h at 873 K to study the phase transformations. A series of $CuO-ZrO_2$ samples with a nominal CuO content from 1 up to 33 mol% were prepared by adjusting the appropriate concentrations of $Cu(NO_3)_2{\cdot}3H_2O$ in the initial solutions. Yttrium-stabilized zirconia samples with and without Cu were also prepared following similar, sol–gel procedure and employing yttrium nitrate as the yttrium source for comparison.

Selected samples were immersed in 70% nitric acid for 12 h to dissolve extra lattice or dispersed CuO particles, washed with deionized water, dried at 373 K for 8–10 h and calcined at 873 K for 6 h. The solids were analysed by X-ray fluorescence (XRF) and the washings were analysed by Atomic Absorption Spectroscopy (AAS) for Cu content.

2.2. Sample characterization

The powder X-ray diffraction analysis was carried out using a Rigaku X-ray diffractometer (Model DMAX IIIVC) equipped with a Ni-filtered Cu-Kα (1.542 Å) radiation and a graphite crystal monochromator. Silicon was used as an external standard. The data were collected in the 2θ range, 25–90° with a step size of 0.02° 2θ and counting time of 15 s at each step. The sample was rotated throughout the scan for better counting statistics. The observed interplanar d spacing was corrected with respect to silicon. The unit cell parameters were determined using the corrected d values and then refined using least-square fitting.

Photoemission spectra were recorded on VG Microtech Multilab ESCA 3000 spectrometer using nonmonochromatized Mg-Kα X-ray source ($h\nu = 1253.6$ eV). Base pressure in the analysis chamber was maintained at $4-8 \times 10^{-8}$ Pa range. The energy resolution of the spectrometer was set at 0.8 eV with Mg-Kα radiation at pass energy of 20 eV. Binding energy (BE) calibration was performed with Au $4f_{7/2}$ core level at 83.9 eV. BE of adventitious carbon (284.9 eV) was utilized for charge correction with $Cu-ZrO_2$. The error in all the BE values reported here is within ± 0.1 eV.

The surface areas (BET) of the samples were determined after degassing the samples at 573 K and analysing the N_2 adsorption isotherm at liquid nitrogen temperature (ASAP 2000 system, Micromeritics). The chemical analysis of the samples was done by atomic absorption and XRF.

Thermal analysis of the samples (non-calcined) was carried out on a 'Rheometric Scientific-STA 1500' for DTA/TGA/DTG measurements. The rate of heating employed was 10 °C/min. The air flow rate was 25 ml/min. The sample weight used was approximately 10 mg. The analysis was carried out from room temperature (30 °C) to 1000 °C.

Impedance measurements on pure sintered copper-stabilized zirconia for various compositions were carried out to determine the various contributions to the total conduction. The measurements were carried out on an 'Impedance/Gain-phase Analyser' (Schlumberger-model SI1260). Measurements were restricted to temperatures of up to 483 K because of the experimental limitations. The frequency range employed was from 10 Hz to 10 MHz.

2.3. Catalytic oxidation of CH_4

The catalytic oxidation of CH_4 was performed in an up-flow, fixed-bed, tubular quartz reactor (0.4 cm diameter and 35 cm in length). Approximately 300 mg of the ground oxide was pressed in the form of a pellet. The pellet was crushed to obtain the catalyst in the form granules (mesh size 0.5–1 mm) and was preheated for 1 h at 723 K in N_2 flow (10 ml/min). After cooling down to 523 K, the sample was exposed to the reaction gas mixture of O_2 (48 ml/min) and CH_4 (12 ml/min) at atmospheric pressure and at a residence time of 0.25 s (gas hourly space velocity of 15,000 h^{-1}). After 20 min, the gas composition at the reactor

exit was determined by an online gas chromatograph (Shimadzu 17A) with thermal conductivity detector (column: C molecular sieve, i.d.: 3 mm, length: 2 m). The conversion of methane was calculated in terms of CO_2 formed. The catalyst was tested with ascending and descending temperatures to study the light-off temperature and catalyst deactivation. The catalytic activity was also studied at various lower residence time to study the mass transfer limitations.

3. Results and discussion

3.1. Sample characterization

$CuO–ZrO_2$ samples with a copper oxide content of 1–20 mol% were light-green to greenish black in colour. The BET surface areas of the samples (calcined at 873 K) were in the range of 2–8 $m^2\ g^{-1}$. Since different types of Cu species exist in these samples, there is no monotonic decrease or increase in the surface area of the samples with increasing Cu content. The multiple XRD patterns of representative samples are given in Fig. 1. Unlike in other techniques, pure zirconia prepared by sol–gel method and calcined at 723 K is predominantly in a metastable cubic structure with a small amount of monoclinic phase, having a higher surface area of 40 $m^2\ g^{-1}$ (Fig. 1a). When it was further heated at 873 K, it transforms to a more stable monoclinic phase. The $CuO–ZrO_2$ samples with CuO content in the range of 2–20 mol% exhibit the cubic fluorite structure even after calcination at higher temperatures (873 K) (Fig. 1b–d). The XRD pattern of the sample with 25 mol% of Cu reveals the presence of some copper oxide phase. This study indicates that Cu content from 2 to 20 mol% in $CuO–ZrO_2$, stabilizes zirconia in the cubic, fluorite structure. The lattice parameter decreases from 5.09 (for pure zirconia) to 5.058 Å as the Cu content increases from 0 to 25 mol%.

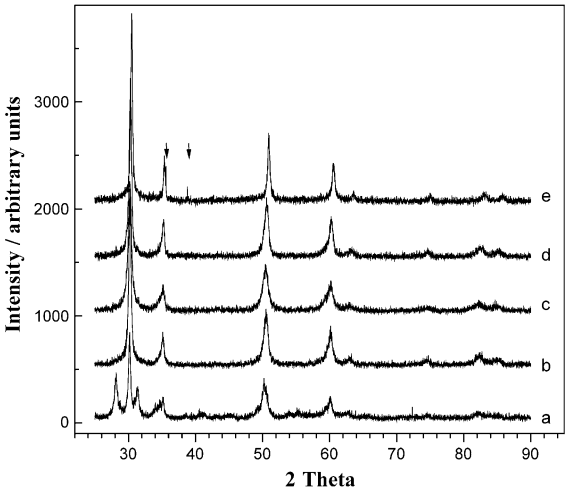

Fig. 1. Powder XRD profiles of ZrO_2 (curve a) and $CuO–ZrO_2$ samples containing 5, 10, 20 and 25 mol% CuO in ZrO_2 prepared by sol–gel procedure and calcined at 873 K (curves b to e, respectively).

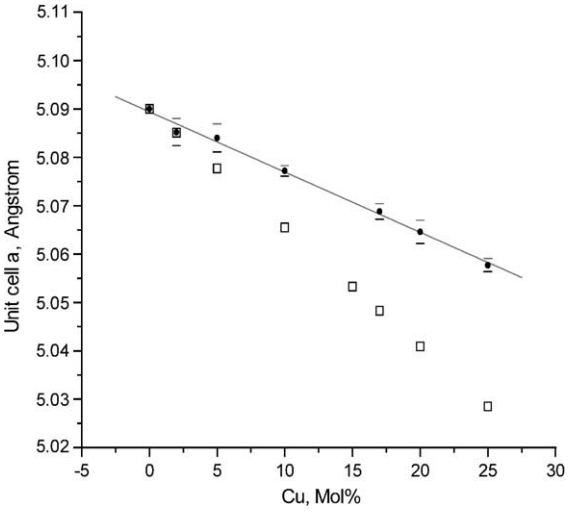

Fig. 2. Variation in cubic unit cell parameters of $CuO–ZrO_2$ samples with increase in copper content. Experimental and theoretical data points are denoted by circle and square, respectively.

Fig. 2 shows the variation of the cubic lattice parameter, which is fairly linear with the copper content in ZrO_2. Also shown in Fig. 2 are the calculated lattice parameters for the known molar concentrations of copper in ZrO_2, assuming substitution of Zr^{4+} (ionic radius = 0.84 Å) in eight-fold coordination by smaller Cu^{2+} ions (ionic radius = 0.72 Å) in six-fold coordination in the cubic lattice. It is seen that there is up to 2% of CuO, the experimental lattice parameter values agree with the calculated values. This indicates the substitution of Zr^{4+} by Cu^{2+} ions in the lattice. As the copper content increases, more Cu^{2+} ions may go into the lattice, but the decrease in lattice parameter does not match

with the theoretical values beyond about 2 mol% CuO in ZrO_2. On a rough approximation, only about half the input copper oxide probably goes into the substitutional position because 5, 10 and 20 mol% CuO samples give lattice parameters equivalent to the values calculated for 2.5%, 5% and 10% CuO assuming that CuO goes into zirconia lattice substitutionally. Since X-ray diffraction does not reveal the presence of CuO as a separate phase up to 20 mol% CuO, the remaining CuO may go into the lattice occupying the interstitial position. As the copper content increases to 25 mol%, the extra copper is precipitated as a second phase as indicated by XRD. It is thus clear that CuO concentration up to 15–20 mol% dissolves in the structure. This is in agreement with the work of Choudhary et al. [5], who reported the stabilization of cubic zirconia by the addition of transition metals. The regression coefficient R, from the least-square fit is -0.9973 for the experimental data, which is extremely satisfactory. The standard deviation of the lattice parameters for all the samples varied from 0.0013 to 0.0028, which is shown in Fig. 2.

The CuO–ZrO_2 samples were further characterized by X-ray photoelectron spectroscopy (XPS) to shed some light on their electronic structure. Fig. 3 shows the photoemission spectra from Cu $2p_{3/2}$ core level at different copper loading. An interesting observation is

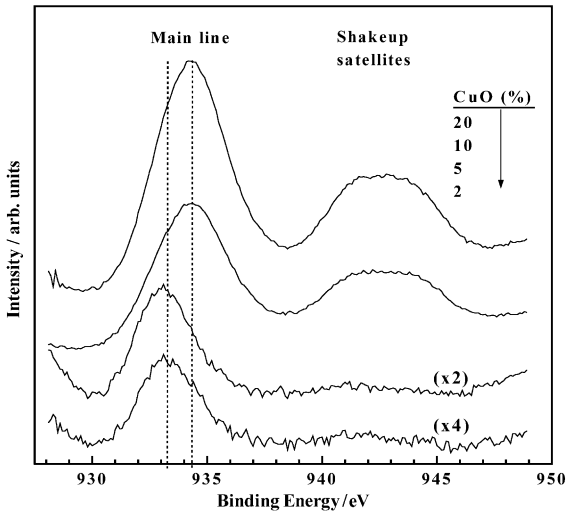

Fig. 3. X-ray photoemission spectra for CuO–ZrO_2 samples with various copper loading recorded at room temperature with Mg-Kα radiation.

that at low copper loadings (≤ 5 mol%), there is only one peak at a BE of 933.3 eV without any satellite at higher BE. However, at Cu levels of ≥ 10 mol%, there is a clear broadening observed with main line and is shifted to higher BE at 934.4 eV. Additionally, it shows a strong satellite in the energy range between 938 and 947 eV. The BE of the main line clearly indicates that the oxidation state of copper species is essentially Cu(II) and it is in good agreement with the values reported in the literature [6–9].

The absence of satellite peaks in CuO–ZrO_2 samples at CuO loading levels of ≤ 5 mol% clearly indicates that there is a very good interaction in terms of charge transfer from nearby oxygen ligands to copper, and hence, the BE of main line is lower than the BE of pure CuO, which appears at 934.1 eV [7]. The low BE associated with this peak also hints that it might be associated with the holes created by oxygen vacancies in the ZrO_2 lattice. The intensity of this peak increases with copper loading. However, there is a high BE feature observed at 934.4 eV with the satellite feature and its intensity also increases from 10 mol% of CuO and above. This feature is essentially the same as that of CuO, except for somewhat higher BE at 934.4 eV and is attributed to CuO dispersed in the lattice. Acid leaching of the above samples does not remove any extra lattice copper and this clearly suggests that the above CuO species could be interfaced with the ZrO_2 lattice. The extra features seen in samples containing ≥ 10 mol% CuO are completely missing in samples with ≤ 5 mol% CuO. This clearly indicates that there may not be any extra lattice CuO in samples containing ≤ 5 mol% CuO, at least on the surface.

The XPS results thus support the findings from XRD. Both techniques show that about half of the input copper goes into the lattice and the remaining should be present as surface and/or subsurface cupric oxide species.

3.2. Thermal analysis

The thermal decomposition behaviour of the copper oxide zirconia precursor gel which dried at 110 °C was studied using DTA/TGA/DTG technique in order to understand the copper zirconia solid solution formation using sol–gel method.

The data are presented in Fig. 4. It is observed that the first endothermic peak is at temperatures varying

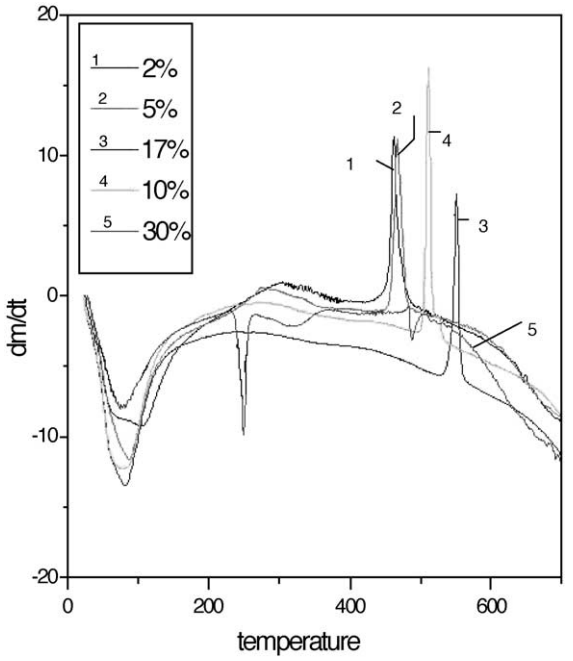

Fig. 4. Variation of DTA curves of copper-stabilized zirconia samples with varying copper concentration.

from 30 to 190 °C with peak values of 82–150 °C, depending upon the CuO content of up to 17 mol%. The peak value decreases with increases in copper content. Another broad endothermic peak is observed between 190 and 350 °C. In this case also, peak temperatures decreased with the increase in CuO content in ZrO_2. Both of these peaks are associated with the weight change varying from 18% to 23% increasing with increasing CuO and from 3% to 8% with weight change decreasing with increasing CuO content. It is suggested that the first endothermic peak is due to the decomposition of copper nitrate to copper oxide while the second is due to the decomposition of zirconium oxy-hydroxide to zirconium oxide. Subsequently, both of these oxides react to form a solution resulting in the exothermic peak without any weight loss observed at peak temperatures varying from 462 to 551 °C, the temperature increasing with increasing CuO content.

It is interesting to note that no exothermic peak is observed for samples containing 30% CuO. It may be noted from XRD reported earlier that this composition indicated the presence of CuO as a second phase. It appears that because of the high concentration of CuO, the exothermic peak is masked by the strong endothermic reactions corresponding to the decomposition of copper nitrate and zirconium oxy-hydroxide.

This is a further confirmation of the earlier results indicated that only up to 17 mol% of CuO goes into solid solution of ZrO_2.

3.3. Complex impedance analysis

In complex plain impedance analysis, the imaginary part Z'' is plotted against the real part Z' for various frequencies. The intercept on the real axis by the semicircular arc can be used to evaluate resistance [10].

The impedance plots show a depressed semicircular arc passing through the origin for all the samples. A typical plot is shown in Fig. 5. These depressed semicircular arcs have θ greater than 10. This suggests the presence of at least two different conduction processes having overlapping time constants close to each other or distribution of time constants for a single process, i.e. there is a distribution of relaxation times.

As a first approximation, the intercept of circular arc in the high frequency side on the real axis may be taken as the value of bulk resistance. Knowing these values and the dimensions of the pellets, bulk specific conductivities have been calculated.

The logarithm of bulk conductivity is plotted in Fig. 6 against reciprocal temperature for each sample. The straight-line behaviour indicates that the Arrhenius relationship is obeyed. The activation energy is then

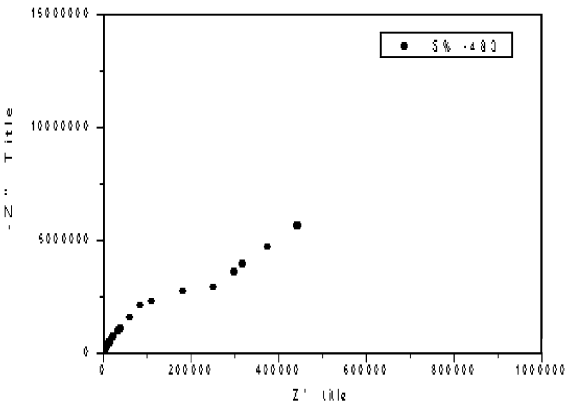

Fig. 5. Impedance plot of 5 mol% CuO–ZrO_2 sample at 483 K.

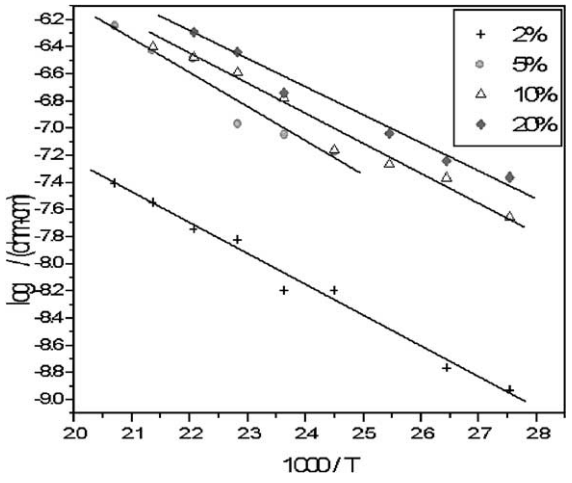

Fig. 6. Logarithm of conductivity of copper-stabilized zirconia with varying concentration as a function of inverse temperature.

calculated from the slopes of these plots. These plots of logarithm of bulk conductivity against reciprocal temperature for various samples are superimposed as shown in Fig. 6. It can be seen from the figure that the conductivity increases with increase in the copper oxide content of the sample. Also, the activation energies of the various samples fairly remain constant even though there is an increase in conductivity as the copper content of the samples increases.

An increase in the conductivity of copper-stabilized zirconia, without any change in the activation energy, suggests that the mechanism of conduction is not altered by the increase in the copper content of the samples. If the copper ion replaces zirconium ion from the lattice of zirconia, the result will be the creation of additional oxygen vacancies in the same way as the ones generated by its replacement by calcium or yttrium ion.

The logarithm of bulk conductivity against sample composition was plotted for a particular temperature (150 °C) as shown in Fig. 7. The figure indicates that the conductivity changes (increases) up to 10 mol% of CuO in zirconia, after which it remains constant. This indicates that only up to 10 mol% of copper goes into substitution position creating oxygen ion vacancies because of the charge imbalance. The zirconia lattice can tolerate only certain concentration of vacancies as observed in calci (50 mol%) and yttria-stabilized zirconia (8 mol%). It is thus clear that the concentration of CuO above 10% does not significantly alter the conductivity, and that the conductivity is predominantly due to the presence of oxygen ion vacancies. Further investigations are necessary to confirm whether the predominant conduction is ionic or electronic.

3.4. CH_4 combustion on $CuO–ZrO_2$

The catalytic activity of $CuO–ZrO_2$ samples in complete CH_4 combustion was studied after calcining the ground powder at 873 K in a quartz reactor. Fig. 8 depicts the catalytic activity for the complete oxidation of CH_4 between 573 and 873 K for $CuO–ZrO_2$ and the single metal oxides (ZrO_2 and CuO) as reference. Pure zirconia and CuO are not as active and only 22% conversion was seen at 873 K. All tested cubic $Cu–ZrO_2$ catalysts proved to be active, leading to a total conversion of CH_4 within 673 and 773 K. Addition of CuO shifts the light-off curves to lower temperature. In every case, CO_2 was the sole product and no carbon monoxide or partial oxidation products were detected during oxidation. For the individual catalysts, the temperature range between an appreciable methane conversion (10–15%) and nearly complete conversion of CH_4 (96–98%) was found to be quite narrow, never exceeding 100 K. Sample containing 20 mol% of CuO showed the best

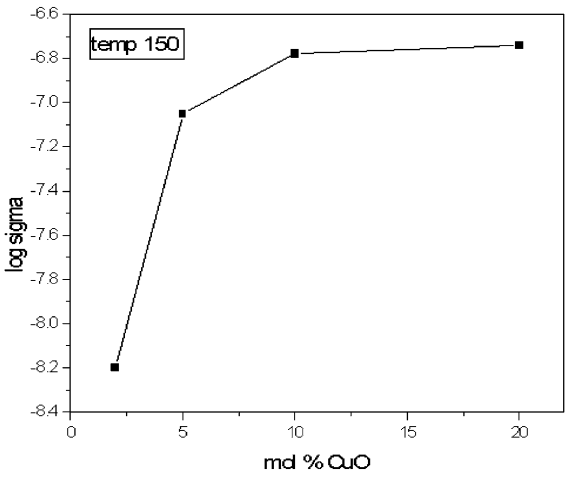

Fig. 7. Variation of logarithm of conductivity of copper-stabilized zirconia with varying copper concentration at 150 °C.

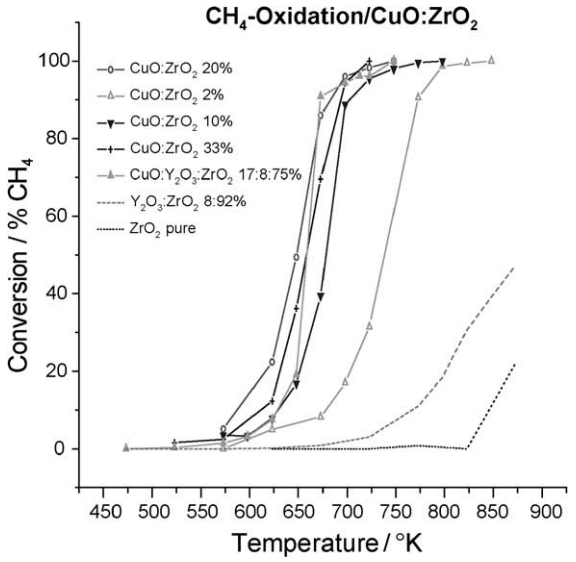

Fig. 8. Catalytic activity of ZrO_2, CuO, Y_2O_3–ZrO_2, CuO–Y_2O_3–ZrO_2 and CuO–ZrO_2 for methane oxidation at a residence time of 0.25 s.

catalytic performance, with 95% conversion at 673 K, among the series under study. The effect of the specific surface area on the catalytic performance is of secondary importance, considering the fact that all the Cu samples have almost similar, low surface areas. A steady increase in catalytic activity of CuO–ZrO_2 samples with CuO content of up to 20 mol% clearly shows that the catalytic activity is related to the CuO species present in the lattice positions as well as on the surface/subsurface layer of cubic ZrO_2. The copper species inside the ZrO_2 lattice may be the most likely one of the catalytically active sites for the oxidation reaction. The catalytic activity of CuO–ZrO_2 (CuO content 20 mol%) sample was also studied at lower residence time than 0.25 s and there was no appreciable change in the catalytic activity. The steep increase in the conversion of methane after light-off is normally associated with autothermal oxidation due to exothermicity of the reaction. With a very small quantity (300 mg) of the catalyst in the microreactor, a temperature raise of about 5 K between the thermocouple inside and outside the reactor was noticed. In this region of autothermal oxidation, the influence of residence time on activity is not perceived to be any different and is probably limited by mass transfer.

The catalytic activity of yttrium-stabilized ZrO_2 containing an equivalent amount of copper is apparently higher than that of the corresponding CuO–ZrO_2. The light-off temperature was 650 K for yttrium-stabilized ZrO_2 with copper oxide, which was lower than for CuO–ZrO_2 (673 K) (Fig. 8). However, without Cu, the yttrium-stabilized ZrO_2 showed very low activity. It is also interesting to note that yttrium-stabilized ZrO_2 (cubic) was comparatively more active than pure ZrO_2 (monoclinic). The higher catalytic activity of the CuO–ZrO_2 with 20 mol% in the system under study is attributed to maximum amount of copper in substitutional position and the resulting oxygen vacancies. The CuO in the lattice position seems to be an active site for redox reaction and oxygen vacancies enhance the catalytic activity because of the higher oxygen mobility in cubic zirconia. The higher activities of yttrium zirconia as compared to pure zirconia (Fig. 8) illustrate the influence of oxygen vacancies and their mobility on catalytic activity. The catalytic activity of CuO–ZrO_2 reported here is somewhat comparable to that reported by Kundakovic and Flytzani-Stephanopoulos [2] where Cu was dispersed on the surface of zirconia. In fact, in both the cases, the 20% Cu-catalysts have similar light-off temperatures, even though there is a large difference in the space velocities (80,000 vs. 15,000 h^{-1}). However, a part of Cu^{2+} ions in the present system is in the substitutional position because of the sol–gel method of preparation. The sol–gel method of preparation has well-known advantages over coprecipitation method and yielded CuO–ZrO_2 samples with stabilized cubic structure. The catalytic activity of CuO–ZrO_2 in complete oxidation of methane was also higher than that of substituted perovskites [11] and perovskite-based catalysts [12]. The enhancement in catalytic activity in total oxidation using perovskite (ABO_3) was correlated with the defect structure and oxygen vacancies created because of substitution of A and/or B site cation. Similar enhancement in catalytic activity in complete oxidation of *n*-butane using Mn-stabilized zirconia has been reported by Keshavaraja and Ramaswamy [13]. The activity for methane oxidation increases until bulk-like CuO is formed on the surface of the solid. Although the observed activity is much higher than that of mixed-metal oxides with zirconia as support and other metal oxides [3,10,14–16], the performance

can even be improved by optimising the calcination conditions.

4. Conclusion

A series of samples of CuO-stabilized zirconia, $CuO–ZrO_2$ with CuO content from 1–33 mol% was prepared by sol–gel procedure. The decreasing unit cell values with increasing CuO concentration supports the incorporation of copper in the lattice position. XPS study of this sample showed that Cu is essentially in the Cu^{2+} oxidation state and incorporates into the zirconia lattice up to 5 mol%. Impedance measurements indicate that the conduction mechanism is not altered by incorporation of CuO in the ZrO_2 lattice. It is suggested that approximately half of the input copper goes into the lattice and the remainder stays as extra lattice copper in samples with CuO content above 5 mol%, supporting the findings from XRD. The incorporation of redox Cu^{2+} active species into the structure of cubic zirconia combined with oxygen mobility due to oxygen vacancies leads to formation of catalysts that are superior to either CuO, ZrO_2 or CuO supported on ZrO_2.

Acknowledgements

The authors would like to thank Ajit Kulkarni, Veda Ramaswamy, C.S. Gopinath and D. Srinivas for their assistance. One of the authors, V.B. Tare, is thankful to AICTE for financial assistance.

The authors gratefully acknowledge the financial support from the Volkswagen-Stiftung (project 1/73 506) enabling the scientific cooperation between two institutions.

References

[1] R.J. Gorte, S. Park, J.M. Vohs, C. Wang, Adv. Mater. 12 (19) (2000) 1465–1469.
[2] Lj. Kundakovic, M. Flytzani-Stephanopoulos, Appl. Catal., A Gen. 171 (1998) 13–29.
[3] R.X. Zhou, X.Y. Jiang, J.X. Mao, X.M. Zheng, Appl. Catal., A Gen. 162 (1997) 213–222.
[4] M.K. Dongare, V. Ramaswamy, C.S. Gopinath, A.V. Ramaswamy, J. Catal. 199 (2001) 209–216.
[5] V.R. Choudhary, B.S. Uphade, S.G. Pataskar, A. Keshavaraja, Angew. Chem. 35 (1996) 2393–2395.
[6] G. Van der Lann, C. Westra, C. Haas, G.A. Sawatzky, Phys. Rev., B 23 (1981) 4369–4380.
[7] K. Allan, A. Campion, J. Zhou, J.B. Goodenough, Phys. Rev., B 41 (1990) 11572–11575.
[8] C.D. Wagner, W.M. Riggs, L.E. Davis, J.F. Moulder, G.F. Muilenberg, Handbook of X-ray Photoelectron Spectroscopy, Perkin-Elmer, Physical Electronics Division, Eden Prairie, MN, 1979, and references therein.
[9] S. Larsson, M. Braga, Chem. Phys. Lett. 48 (1977) 596–600.
[10] J.R. Macdonald (Ed.), Impedance Spectroscopy, Wiley, New York, 1987.
[11] H. Arai, T. Yamade, K. Eguchi, T. Seiyama, Appl. Catal. 26 (1986) 265–276.
[12] S. Cimino, L. Lisi, R. Pirone, G. Russo, M. Turco, Catal. Today 59 (2000) 19–31.
[13] A. Keshavaraja, A.V. Ramaswamy, Appl. Catal., B Environ. 8 (1996) L1–L7.
[14] K. Tanabe, T. Yamaguchi, Catal. Today 20 (1994) 185–198.
[15] Y. Okamoto, H. Gotoh, H. Aritani, T. Tanaka, S. Yoshida, J. Chem. Soc., Faraday Trans. 93 (1997) 3879–3885.
[16] F. Zamar, A. Trovarelli, C. de Leitenburg, G. Dolitti, J. Chem. Soc., Chem. Commun. 9 (1995) 965–966.